



Fermi National Accelerator Laboratory

A Department of Energy National Laboratory

Managed by Universities Research Association

**DESIGN OF MECHANICAL SYSTEM AND TOOLING FOR STAVE  
INSTALLATION INTO D0 RUN IIB SILICON DETECTOR**

**THERMAL PERFORMANCE OF COOLING TUBES FOR  
D0 RUN IIB SILICON DETECTOR STAVES**

LUDOVICO P. LORANDI

MECHANICAL AND INDUSTRIAL ENGINEERING DEPARTMENT

THE UNIVERSITY OF TEXAS AT EL PASO

EL PASO, TX 79968

SUPERVISOR: DANIEL R. OLIS

PARTICLE PHYSICS DIVISION MECHANICAL DEPARTMENT

FERMI NATIONAL ACCELERATOR LABORATORY

BATAVIA, IL 60510

AUGUST 7, 2003

## ABSTRACT

This paper discusses two separate projects related to the upgrade of the D0 silicon detector. First, it addresses the design of a mechanical system and tooling to aid in the installation process for D0 Run IIb silicon detector. The discussion of this design begins with the origin of the idea, and shows the actual progress made. Finally, the paper, in the first part, illustrates with images the actual status of the project.

The second part of this paper is oriented to the discussion of a thermal performance test performed on the cooling tubes for D0 Run IIb silicon detector staves. This part of the paper addresses the purpose of the experiment, the experimental setup and procedure, and, finally, analyses the obtained results for the thermal expansion coefficient of the tube and the force change per unit temperature change that will be experienced by the tube.

## INTRODUCTION

Over the years, Fermilab has committed to the in-depth study of the physics of matter. In doing so, the study and understanding of particle physics beyond the Standard Model has led to many discoveries and innovations. One of Fermilab's main goals today is to discover the Higgs boson and understand the behavior of other important subatomic particles that play an important role in the structure of matter. The most important information source for these studies is the collision of high energy proton and anti-proton beams in the Tevatron collider. These beams are accelerated with alternating electric fields in the Linear Accelerator (LINAC) and the Main Injector prior to their entrance to the Tevatron collider at a speed that is close to 70% the speed of light. The beams travel in opposite directions on a helix pattern and are bent with the aid of a magnetic field. The most important projects in the Tevatron collider are D0 and CDF, which are the two collision sites.

The D0 project, in Run II, is currently using a silicon tracker able to withstand an integrated luminosity of  $4\text{fb}^{-1}$ ; luminosity is a measure of the number of proton to antiproton collisions. Running the collider at higher luminosity will bring greater possibilities for subatomic particle sightings. A projected extension of Run II in the Tevatron collider would deliver an integrated luminosity of  $15\text{fb}^{-1}$ . However, this higher amount of integrated luminosity will produce enough radiation to permanently damage the actual silicon tracker, making it inoperable. Therefore, in order to fully exploit the

physics potential of the Tevatron, it is necessary to design a silicon detector able to withstand high radiation to replace the existing silicon detector. The Mechanical Department of the Particle Physics Division at the Silicon Detector (SiDet) Center is responsible for the design and manufacture of the new silicon detector for D0's Run IIb. This new design represents a great challenge to SiDet's Mechanical Department as it must be fully developed in less than 3 years and must comply with several design constraints in key features such as size, mass, materials, assembly tolerances and resistance to radiation damage.

The proposed silicon detector has a six layer sensor geometry in a barrel design. It will be built in two independent barrel assemblies joined end to end. The 6 layers are divided into two radial groups and are numbered from 0 to 5. The inner group consists of layers 0 and 1, with layer 0's innermost sensor located at a radius of 18.6 mm from the center of the beam line. The outer group, consisting of layers 2-5, shown in Figure 1, will use stiff stave support structures, shown in Figure 2, on which the sensors will be mounted. There will be a total of 128 staves in layers 2-5. Due to the high number of staves that need to be inserted into the relatively small area of the barrel assemblies, the risk of damaging a stave or one of its components, such as the sensors, is increased. To reduce this risk, it is necessary to develop a cautious and effective method for the insertion of the staves into the barrel assemblies.

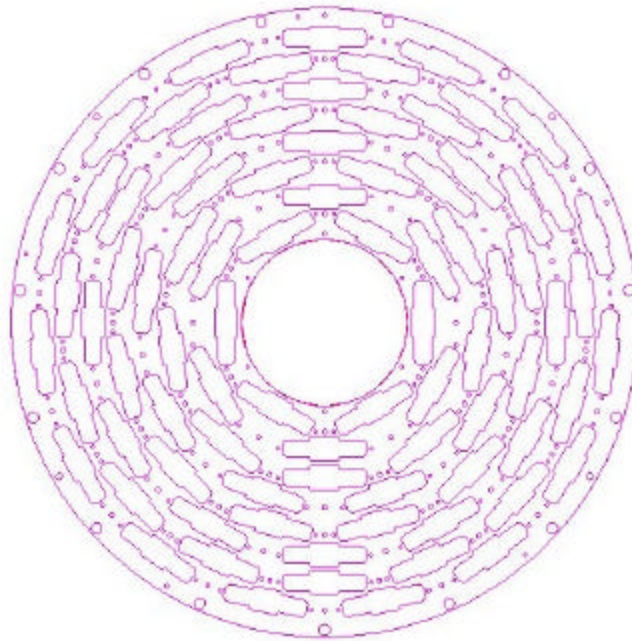


Figure 1 – Front view of  $z=600$  end bulkhead. Stave orifices for layers 2-5 (2A, 2B, 3A, 3B, 4A, 4B, 5A and 5B). 2A is the innermost layer and 5B is the outermost.



Figure 2 – Isometric view of stiff stave. Left end is  $Z=600$  and right end is  $Z=0$ . Bundle wires will be attached at each of the hybrid chips. Cooling tubes will be attached at  $Z=600$  end manifolds.



Figure 3 – Isometric view of barrel assembly. With  $z=600$  end in front and  $z=0$  end in the back.

In addition, a project of such dimension requires the involvement of physicists, engineers and technicians, who have the responsibility of designing, modeling and testing the different components of the new silicon detector.

As SIST Intern, under the supervision of the Silicon Detector Center's Mechanical Department, I was handed the responsibility of designing a mechanical tooling system that would aid the insertion of staves into barrels. I also measured the thermal properties of the stave cooling tubes to verify the thermal expansion coefficient.

## **DESIGN OF MECHANICAL SYSTEM AND TOOLING FOR STAVE INSTALLATION INTO D0 RUN IIB SILICON DETECTOR**

Every day, the design of D0's Run IIB Silicon Detector is improved and it moves closer to its final design. At this stage, it is necessary to consider the detector's installation, in order to ensure the project's success. The high number of staves that need to be installed in the detector calls for the design of a mechanical system capable of installing the staves in a precise and careful manner.

The installation process is delicate because of the highly sensitive components of the staves. Each stave contains silicon sensors and electronic chips. In addition, the presence of bundle wires and cooling tubes requires taking extra precautions in their handling.

The design of the mechanical system for stave installation needs to comply with required design constraints. The barrel is to remain fixed at a location and will be supported horizontally by a 'cradle'. Rotation is not allowed for the barrel or its supporting cradle as it is desired to eliminate dynamic stresses in the barrel and staves. The mechanical system and tooling to be designed should be simple enough to allow the installation process to be done by hand. The installation process should follow a pattern from starting from the outer layers, so that the bundle wires and cooling tubes can hang out without obstructing the entrance orifice to other staves. Also, a supporting rod, to guide the stave through the barrel, should be stiff enough so that, when sliding from  $z=0$  end to  $z=600$  end, won't deflect more than 0.125 in, in order to fit the opening at  $z=600$ .

### **Model Description**

A design of the mechanical system for stave installation to comply with the stated boundary conditions has been developed and it is shown in Figure 4. It is a picture of the 3-D model developed using SDRC-IDEAS software. After brainstorming and discussion of ideas, it was proposed to use a rotating disk, aligned to the barrel, to insert the staves into the silicon detector. Also, it was decided to hold the  $z=0$  end of the stave with a gripping tool attached to a rod, while the  $z=600$  end of the stave would be handheld to obtain a better feedback during insertion. The disk is supported by a plate and it rests on three bearings that allow rotation. To position the disk properly aligned to the barrel, the supporting plate is fixed to two sliders that are mounted on a rail, this mechanism allows the assembly to move horizontally. The rail assembly is fixed to a die set that permits vertical displacement with the aid of a jack.

The stave insertion tooling is constructed from the above mentioned parts and assemblies and will be described in a more detailed manner.

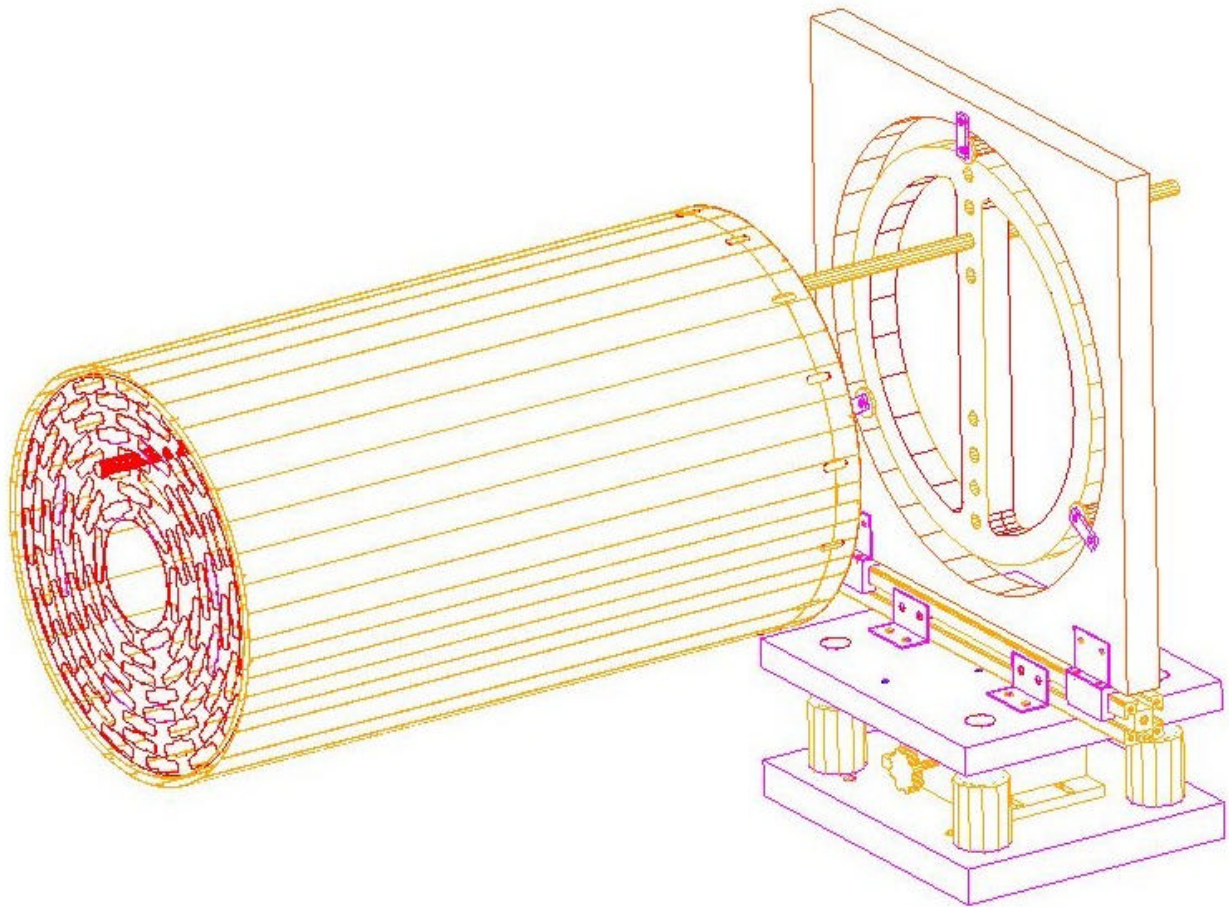


Figure 4 – Mechanical system and tooling designed for stave insertion. D0's silicon detector barrel assembly included.

### **Rotating Disk**

The rotating disk is made of aluminum and has a diameter of 14" and is 1" thick. It is shown in Figure 5. It has eight drilled holes located at different radii, each one corresponding to each of the silicon detector's layers. In order to improve the visibility from the back of  $z=0$  end through the barrel and to reduce the mass of the mechanism, it is necessary to remove as much material as possible. In this case, the disk has two hollow spaces, having a strip of material going through the middle and the perimeter ring. The corresponding holes for each layer lie in that strip of material, as shown in the figure. Also, Figure 5 illustrates the actual geometry of the disk.

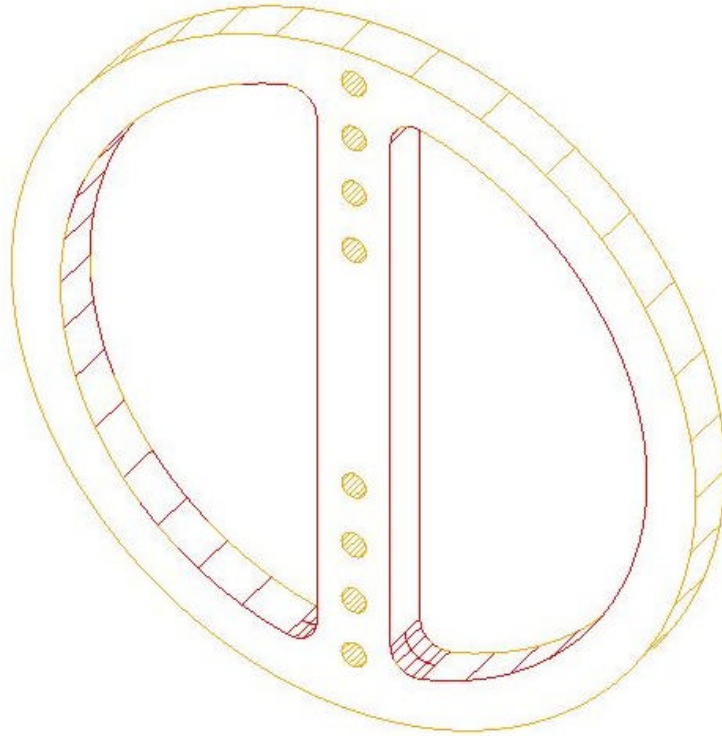


Figure 5 – Isometric view of rotating disk (14” diameter, 1” thickness).

### **Supporting Plate Assembly**

The supporting plate assembly is shown in Figure 6. It consists of an 18” x 18” plate with a 16” diameter hole in the middle, three 5/8” bearings, six aluminum links to hold the bearings and four angled joints that maintain the supporting plate fixed to the rail assembly. Figure 6 shows the supporting plate assembly holding the rotating disk in place. The bearings, shown in Figure 7, will be manufactured at SiDet. This supporting plate assembly is to be mounted on a rail that will allow for horizontal displacement.

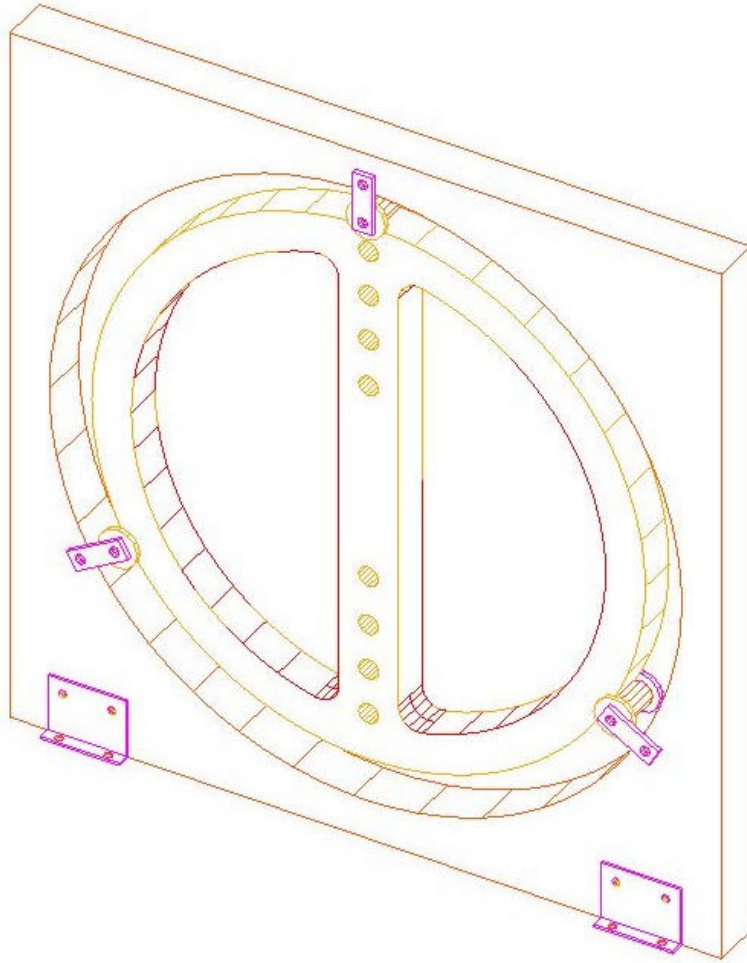


Figure 6 – Isometric view of supporting plate assembly and rotating disk.

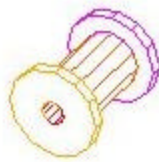


Figure 7 – Isometric view of bearing to be manufactured.

### **Rail Assembly**

The rail assembly consists of a 2” x 2” structural rail by Thorlabs, Inc., two sliding blocks that are attached to the supporting plate assembly and four angled joints to maintain the rail assembly fixed to the die set. Figure 8 shows the rail assembly. The sliding blocks are shown in detail in Figure 9. The sliding block has four #8 holes on its top surface to attach to the supporting plate assembly.

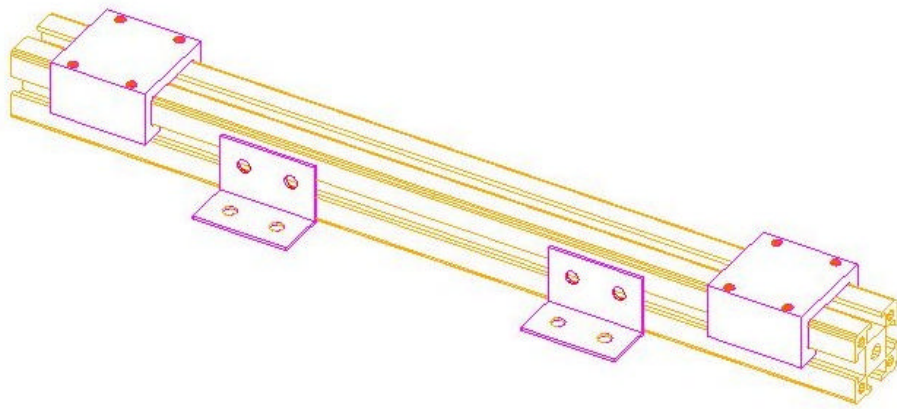


Figure 8 – Isometric view of rail assembly.

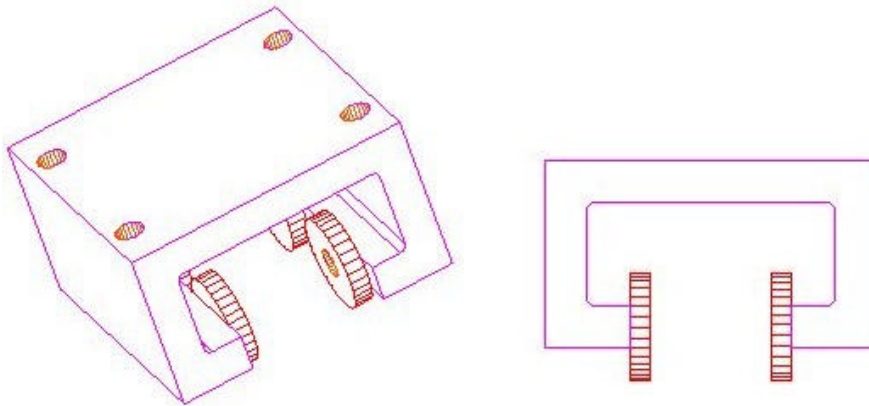


Figure 9 – Isometric and Front view of sliding block.

### Die Set Assembly

The die set assembly consists of a die set and a Newport Lab Jack. The punch holder from the die set (top block) has a pattern of 8 holes for 1/4" threads to hold the rail assembly. The die set assembly is shown below in Figure 10. This assembly will allow the system to move vertically to achieve alignment between the centerlines of both the barrel and the rotating disk.

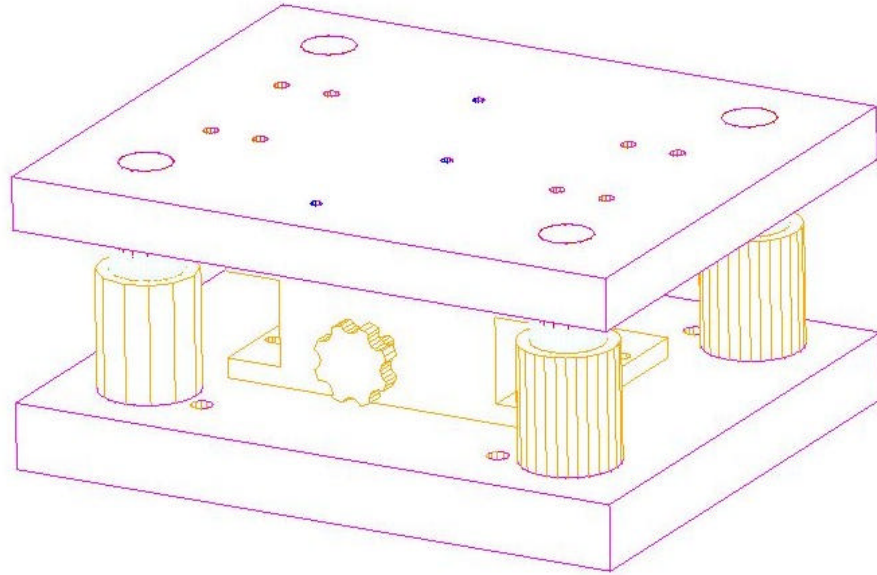


Figure 10 – Die set with Newport Lab Jack.

### **Rod Assembly**

The rod assembly consists of two 7/16" diameter carbon fiber rods. The main rod will be 33" long and has a hole for a #4 thread in one of its faces, as shown in Figure 11. The second rod is 6" long and has a #4 screw to be attached to the main rod and will have a gripping tool, yet to be designed, to hold the stave. The rod is detachable because when the stave approaches to the  $z=0$  end of the barrel won't be perfectly aligned to the corresponding pinholes, so its position should be corrected manually.



Figure 11 – Rod assembly.

To select the proper rod for this model, it was necessary to perform a theoretical deflection analysis on a list of possible rods, varying diameters and material. Three options were considered for the material of the rod: aluminum, steel and carbon fiber. The diameters to be considered were in the range from 1/4" to 7/16". The formula used to carry out this analysis was the cantilever beam equation:

$$d = \frac{-PL^3}{3EI} \quad (1)$$

where  $d$  is the maximum deflection,  $P$  is the load (weight of stave),  $L$  is the length of the rod,  $E$  is the modulus of elasticity of the material and  $I$  is the area moment of inertia of the cross section.

The best option for this application was a 7/16" diameter carbon fiber rod. The analysis is shown in the following tables.

Deflection of Unloaded Rod (in)				
Material	Diameter (in)			
	1/4"	5/16"	3/8"	7/16"
Aluminum	0.3711	0.1520	0.0733	0.0396
Steel	0.3592	0.1471	0.0710	0.0383
Carbon Fiber	0.0776	0.0318	0.0153	0.0083

Table 1 – Deflection caused by the rod's own weight.

Deflection with Stave Loading (in)				
Material	Diameter (in)			
	1/4"	5/16"	3/8"	7/16"
Aluminum	2.2490	0.1520	0.0733	0.0396
Steel	0.7497	0.3071	0.1481	0.0799
Carbon Fiber	0.7497	0.3071	0.1481	0.0799

Table 2 – Deflection caused by the weight of the stave, not considering the rod's own weight.

Total Deflection (in)				
Material	Diameter (in)			
	1/4"	5/16"	3/8"	7/16"
Aluminum	2.6201	1.0732	0.5176	0.2794
Steel	1.1089	0.4542	0.2190	0.1182
Carbon Fiber	0.8273	0.3389	0.1634	0.0882

Table 3 – Total deflection of the rod is the sum of the unloaded case and the stave loading case.

## **Conclusion**

The objective of this project was to start the designing process of the tooling required for the stave installation into D0's Run IIb Silicon Detector. However, a design project of this magnitude could not be fully completed in a period of five weeks. As mentioned above, few additions need to be made in order to complete the design. A key feature that needs to be designed is the gripping tool that will be attached to the rod assembly to hold the stave at its  $z=0$  end, in order to guide it through the barrel. However, this project has served well as a starting point in the installation process for the new silicon detector.

## **THERMAL PERFORMANCE OF COOLING TUBES FOR D0 RUN IIB SILICON DETECTOR STAVES**

### **Purpose**

As the design process of the staves for the D0 Run IIB silicon detector advances, it is necessary to investigate the external forces that may be exerted on the detector. The detector's expected operational temperature is of approximately ten degrees Celsius below freezing point. Therefore, it is required to investigate the mechanical behavior of Cilran (SEBS, manufactured by Randolph-Austin) tubes at low temperatures. Also, it is necessary to determine the forces that will be caused by the contraction of the tube due to thermal effects. The Cilran tube is the primary candidate to connect silicon structures to cooling manifolds in Run IIB.

### **Setup**

The setup for the experiment is shown in figure 12. One end of the tube is constrained while the other end is connected to a force gage. The force gage (Chatillon DFIS 10) is mounted on a slide with a scale to read length of travel. Each end of the tube is connected to the fixture with two barb fittings. Each fitting has a fluid passage to allow cooling of the tube with circulating coolant. Flow through the tube goes in at the top and out at the bottom. The chiller (FTS Systems SiDet) feeds the cooling mixture (42% ethylene-glycol by volume in water) that will cause the tube to contract. The temperature is monitored using an RTD at the inlet and outlet of the tube.

### **Procedure**

1. Cut a 12 inch long 5/16" OD, 3/16" ID Cilran (SEBS, manufactured by Randolph-Austin) tube.
2. Connect the tube to the fixture as shown in figure 1.
3. After connecting the tube, add a 0.75lb preload.
4. Cool the tube from 20°C to -20°C. Record the force on the tube at 5°C increments, after reaching steady state.
5. Shut off the flow through the tube, allowing a gradual warming of the tube to room temperature. Record the force every 5°C.
6. With the flow through the tube still shut off, set the coolant temperature at -10°C.
7. Record force with tube at room temperature.

8. Restore flow through the tube to allow rapid cooling from room temperature to -10°C. Record the force.
9. With the tube at -10°C in steady state, stretch the tube 0.1in in 0.025in increments. Record the force at every stage, initially and every minute after for five minutes.



Figure 12 – Experimental setup. Cilran tube connected to force gage and chiller.

## Analysis and Results

A thermal test was conducted on a 12 inch long Cilran tube to measure contracting forces that may occur when exposed to low temperatures. These tests were done to determine the thermal expansion coefficient and modulus of elasticity of the tubing.

Results from test procedures 4 through 8 were used to calculate the quantity  $Ea$  of the Cilran tube. Results from test procedure 9 were used to determine the modulus of elasticity  $E$  of the tube at -10°C, the expected operating temperature of the detector.

To calculate the thermal expansion coefficient consider the following strain relationships:

Mechanical Strain:

$$\mathbf{s} = E * \mathbf{e} \qquad \mathbf{s} = \frac{F}{A} \qquad (2, 3)$$

where  $\mathbf{s}$  is the normal stress,  $E$  is the modulus of elasticity,  $F$  is the axial load,  $A$  is the area of the tube perpendicular to the force and  $\mathbf{e}$  is the strain. Combining equations 2 and 3 and solving for the axial load yield

$$F = E * A * \mathbf{e} \qquad (4)$$

Thermal Strain:

$$\mathbf{e} = \frac{\Delta L}{L} = \mathbf{a} * \Delta T \qquad (5)$$

where  $L$  is the length of the tube;  $\Delta L$  is the change in length that would have occurred were the tube unconstrained;  $\mathbf{a}$  is the coefficient of thermal expansion; and  $\Delta T$  is the change in temperature. Combining equations 4 and 5, an expression for the force on a constrained tube due to thermal effects is obtained:

$$\Delta F = -A * E * \mathbf{a} * \Delta T \qquad (6)$$

Using experimental data it is possible to calculate the average rate of change  $\frac{\Delta F}{\Delta T}$ , so, by rearranging equation 6, the following equation is obtained:

$$E * \mathbf{a} = -\left(\frac{\Delta F}{\Delta T} * \frac{1}{A}\right) \qquad (7)$$

To calculate  $\mathbf{a}$ , a mechanical strain test is required to calculate the modulus of elasticity of the material. Using the data to produce a stress-strain plot, shown in Figure 14, the modulus of elasticity is calculated from equation 2 ( $E$  is the slope of the line).

To obtain the value for the product  $E * a$ , the area of the tube and the ratio  $\frac{\Delta F}{\Delta T}$  must be calculated. The value of  $\frac{\Delta F}{\Delta T}$  is given by the slope of the line in figure 13a and 13b. The rapid cool down test shown in figure 13b demonstrates the time independence of these properties.

$$A = \frac{\pi}{4}(D_o^2 - D_i^2) = \frac{\pi}{4}[(0.313in)^2 - (0.188in)^2] = 0.0492in^2$$

$$\frac{\Delta F}{\Delta T} = -0.012 lb/^\circ C$$

Substituting into equation 7 yields

$$E * a = \left( \frac{-0.012 lb/^\circ C}{0.0492in^2} \right) = 0.245 psi/^\circ C = 0.136 psi/^\circ F$$

Calculating the slope of the lines in figure 14 yields the value of the modulus of elasticity. The maximum force and the force at steady state were recorded. The steeper curve represents the initial force recorded with a step change in tube length. The second curve shows the steady state load reached at steady state after the tube relaxed. The tube reached the steady state condition approximately 1 minute after each incremental stretch. The slope of the steady state conditions was used to determine  $E$  at  $-10^\circ C$ . Substituting that value in the following expression gives the value for  $a$  :

$$E = 1703 psi \quad a = \frac{E * a}{E} = \frac{0.136 psi/^\circ F}{1703 psi} = 7.99 * 10^{-5} /^\circ F$$

By manipulation of the equations it is shown that the force generated from a change in temperature is independent of tube length, as shown in equation 6.

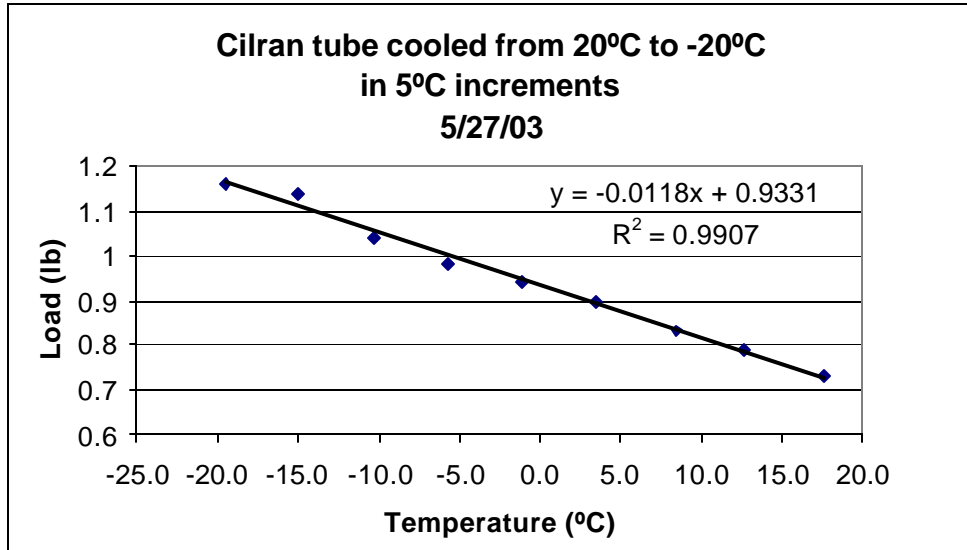


Figure 13a – Load increment on Cilran tube during the cooling process.

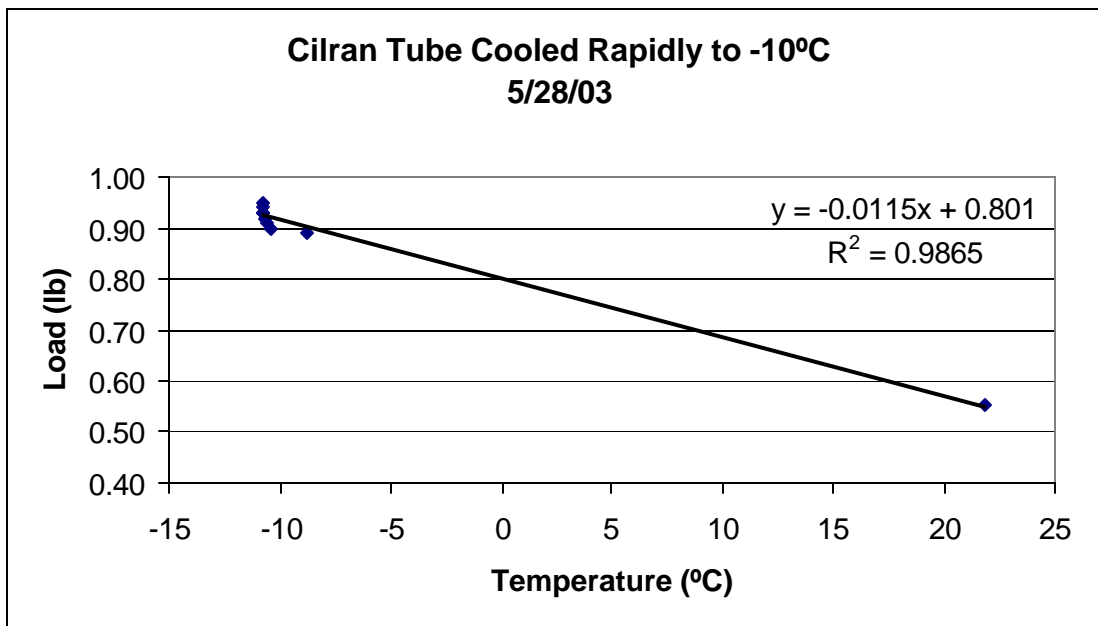


Figure 13b – Load increment on Cilran tube during rapid cooling process.

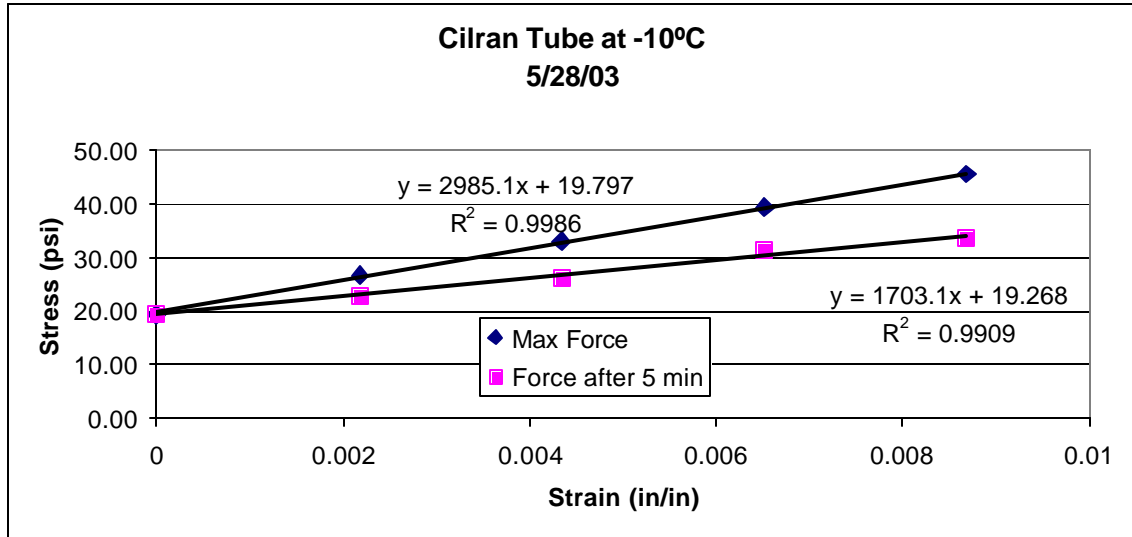


Figure 14 – Stress-strain plots for maximum force (initial) and force at steady state (after 5 minutes). Cilran tube tested at -10°C.

## Conclusion

This experiment was performed to obtain information on the behavior of a Cilran tube when subjected to low temperatures. The experiment proved that the calculation of the thermal expansion coefficient is independent of the cooling time. In addition, the tubing will exert, when added all together, a significant amount of force to the barrel's bulkhead. Therefore, it is necessary to consider installing excess length of tubing so that it is not stretched before the temperature change, reducing the amount of force due to the contraction of the tube.

## **ACKNOWLEDGEMENTS**

I would like to thank all the individuals who made possible for me to write this paper. First of all, I would like to thank my supervisor, Daniel Olis, for his guidance and support throughout the summer. Also, I would like to thank Jim Fast, Giobatta Lanfranco, Frank McConnolongue and Kenneth Schultz for their help and valuable advice. Finally, I would like to express my most sincere gratitude to Mrs. Dianne Engram, Elliot McCrory and James Davenport for giving me the opportunity to have a great and valuable experience at Fermilab.

## **BIBLIOGRAPHY**

- Beer, Ferdinand P. and Johnston, E. Russell, "Mechanics of Materials". McGraw-Hill, Inc., First Edition, 1981
- Budynas, Richard G. and Young, Warren C., "Roark's Formulas for Stress and Strain". McGraw-Hill, Inc., Seventh Edition, 2002
- D0 Collaboration, "D0 Run IIb Silicon Detector Upgrade Technical Design Report". September 12, 2002